



# High temperature steam oxidation of $\text{UO}_2$ fuel pellets

M. Imamura<sup>\*</sup>, K. Une

*Nippon Nuclear Fuel Development Co., Ltd., 2163, Narita-cho, Oarai-machi, Higashi-Ibaraki-gun Ibaraki 311-13, Japan*

## Abstract

In order to evaluate the behavior of steam oxidation of  $\text{UO}_2$  pellets after the occurrence of primary failure, steam oxidation tests were conducted from 800–1200°C in various atmospheres of  $\text{H}_2\text{O}$ ,  $\text{H}_2/\text{H}_2\text{O}$  or  $\text{H}_2\text{O}_2/\text{H}_2\text{O}$ , using unirradiated and irradiated  $\text{UO}_2$  pellets. The change in O/U ratio was analyzed by means of a surface reaction controlled model and the oxidation rate was formulated in terms of exposure time, surface-to-volume ratio and temperature. The effects of liberated hydrogen and hydrogen peroxide on the steam oxidation of  $\text{UO}_2$  fuels were evaluated. The presence of small amounts of hydrogen in the steam decreased only the equilibrium O/U ratio, due to the low oxygen potential in this atmosphere, but had no effect on the surface exchange coefficient. On the other hand, when the concentrations of hydrogen peroxide in water were more than 10 vol.%, the surface exchange coefficient was one order of magnitude higher than in pure steam. The steam oxidation process of the irradiated pellets was also controlled by a reaction at the solid/gas interface. The surface-to-volume ratio of irradiated  $\text{UO}_2$  pellets, which was evaluated from the measured oxidation curves, was approximately 2.6 times that of unirradiated fuel pellets. © 1997 Elsevier Science B.V.

## 1. Introduction

When a Zircaloy-clad fuel rod fails from various causes, such as primary hydriding, debris fretting, pellet-cladding interaction (PCI) or crud induced localized corrosion (CILC), coolant water enters into the fuel rod through small leaks to equalize the pressure difference between the coolant and rod interior. In BWR fuel rods, the water will boil during its passage through the leak opening and the vapor will fill the fuel-cladding gap and the plenum. The entered steam reacts with both  $\text{UO}_2$  fuel pellets and the inner wall of the cladding to liberate hydrogen. From the results of detailed PIEs for defective fuel rods, fuel oxidation was found to play an important role in the generation of hydrogen in comparison with Zircaloy-2 cladding oxidation [1].

Bittel et al. [2] studied steam oxidation of  $\text{UO}_2$  at temperatures from 1158–2108 K. Based on evidence from X-ray diffraction and chemical analyses of an oxygen gradient across the sample, they assumed that the solid-state

diffusion was the rate-controlling process. However, subsequent studies have shown that the rate of oxidation of  $\text{UO}_2$  by steam is governed by kinetics of  $\text{H}_2\text{O}$  decomposition on the surface of the oxide [3,4]. At temperatures less than 1800 K, the reaction is slow compared to solid-state diffusion of oxygen and the surface chemical kinetics is thus rate-controlling. Abrefah et al. [5] studied the steam oxidation behavior of unirradiated  $\text{UO}_2$  fuel pellets by using a thermogravimetric apparatus in the temperature range 1273–1623 K at one atmosphere for the system pressure. Lewis et al. [6] carried out steam oxidation tests of irradiated fuel pellets and obtained high temperature data above 1200°C on fission products release. Models for the evaluation of fission gas release from defective fuel rods have also been reported [7,8]. But there are no steam oxidation experiments at the low temperatures found near the surface temperatures of pellets and there are no experiments on the effects of the gap atmosphere. In failed rods, released hydrogen and radiolysis compounds such as hydrogen peroxide must coexist together with steam. Therefore, accurate knowledge of the oxidation rate of  $\text{UO}_2$  pellets under various atmospheres is needed to evaluate quantitatively the scenario for deterioration of failed rods. In this report, the effects of several atmospheres on the

<sup>\*</sup> Corresponding author. Tel.: +81-29 266 2131; fax: +81-29 266 2589; e-mail: imamura@nfd.co.jp.

steam oxidation were evaluated using unirradiated fuel pellets. Steam oxidation experiments using irradiated pellets were also conducted.

## 2. Experimental

### 2.1. Fuel specimens

Unirradiated and irradiated  $\text{UO}_2$  fuel pellets were used for steam oxidation experiments. The unirradiated fuel specimens,  $1 \pm 0.01$  mm cubes, used in steam oxidation tests were cut from the sintered pellets of about 10 mm height and 10 mm diameter by using a slicing machine. As-sintered density of the unirradiated  $\text{UO}_2$  pellets was 97% of the theoretical density. Three-dimensional grain size was 16  $\mu\text{m}$ . O/U ratio of unirradiated  $\text{UO}_2$  pellets before steam reaction tests, as measured by polarography, was 2.005. The surface-to-volume ( $S/V$ ) ratio of specimens, as measured by the BET method, was  $210.5 \text{ cm}^{-1}$ . The irradiated specimens were prepared from  $\text{UO}_2$  fuel pellets irradiated in a commercial BWR, to a burnup of 27  $\text{GWd/tU}$ . The fuel specimens, about 1 mm cubes, were taken from the outer region of the irradiated pellets. Several cubes of both unirradiated and irradiated  $\text{UO}_2$  were used in the steam oxidation tests.

### 2.2. Steam oxidation tests

Fig. 1 shows a schematic diagram of the pellet–steam oxidation system used in this study. This device consists of a microbalance, a steam generator, an electric furnace and a steam condenser. The weight change as a function of time was measured by a Perkin–Elmer microbalance. The  $\text{UO}_2$  fuel specimens were hung from the microbalance using a platinum wire at approximately the center of the hot zone of the electric furnace. The  $\text{UO}_2$  fuel specimens

were heated to a fixed temperature in the various atmospheres. Steam was generated by a boiler connected to the furnace by a stainless steel line that was heated to prevent condensation. Steam partial pressure was controlled in the steam generator by keeping a fixed temperature. The dew point of steam was  $50^\circ\text{C}$ . High purity Ar gas was used as carrier gas. The average steam flow rate was approximately  $400 \text{ cm}^3/\text{min}$ , which was controlled by a flowmeter.

### 2.3. Microstructural observations and oxygen analyses

After the steam oxidation tests, specimens were mounted in resin and polished. Detailed microstructural features were examined on polished specimen surfaces by optical and scanning electron microscopies (SEM). The magnification was  $\times 500$  for the former, and  $\times 1000$  to  $\times 3000$  for the latter. The fuel oxidation (O/U ratio) at local sites, on a micron scale, was analyzed by EPMA. The measurement conditions were as follows: acceleration voltage, 20 kV; specimen current, 100 nA; beam diameter, 1  $\mu\text{m}$ . Under these conditions, the effective analysis area was broadened to 2–3  $\mu\text{m}$ . The local O/U ratio in the steam oxidized specimens was derived by using a previously obtained correlation of the characteristic X-ray intensity ratio of oxygen to uranium by EPMA and the O/U ratio by polarography. As unirradiated standard specimens,  $\text{UO}_{2+x}$  ( $x = 0\text{--}0.22$ ) pellets and a  $\text{U}_3\text{O}_8$  (O/U = 2.67) powder compact were used. The error in evaluating the local O/U ratio was expected to be  $\pm 0.005$ .

## 3. Results and discussion

### 3.1. Oxygen potential and equilibrium O/U ratio

In failed rods, hydrogen due to the reactions of steam with  $\text{UO}_2$  pellets and the inner wall of the cladding and

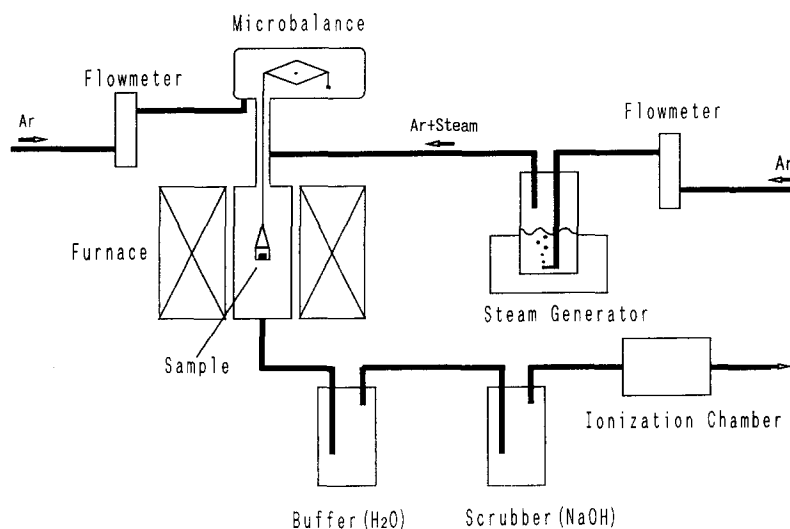


Fig. 1. Schematic drawing of steam oxidation system.

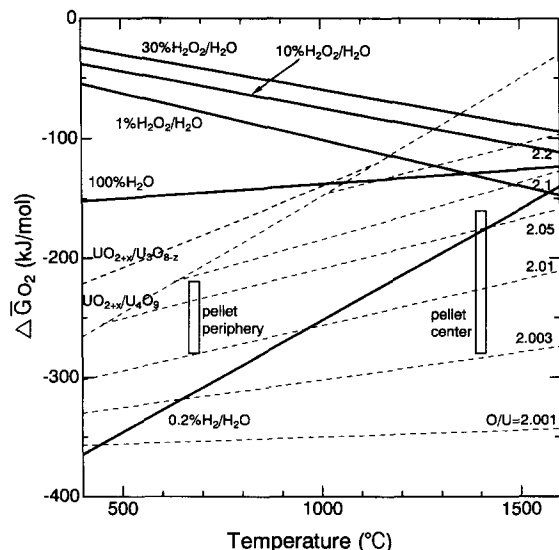


Fig. 2. Oxygen potentials of various atmospheres and  $\text{UO}_{2+x}$ .

radiolysis compounds, such as hydrogen peroxide, must coexist together with steam.

Ar–0.2%  $\text{H}_2$  gas was used as carrier gas to evaluate the influence of the liberated hydrogen on the steam oxidation. Fig. 2 shows the oxygen potentials of the 0.2%  $\text{H}_2/\text{H}_2\text{O}$  mixture and unirradiated  $\text{UO}_{2+x}$  pellets. The average temperatures of the pellet periphery and center regions calculated by a fuel performance code and the O/U ratio measured for defective irradiated fuel pellets are super-imposed on Fig. 2 [1]. From the figure, the atmosphere for the 0.2%  $\text{H}_2/\text{H}_2\text{O}$  mixture is almost the same as that in the defective rods at the end of irradiation. Oxygen potential is  $-215$  kJ/mol at  $1200^\circ\text{C}$  and the equilibrium O/U ratio in this atmosphere is calculated as 2.014.

To evaluate the effect of hydrogen peroxide on steam oxidation behavior, steam containing various amounts of hydrogen peroxide was used. The concentration of hydrogen peroxide in the recirculation pipes in BWR is believed to be several hundred ppm [10]. However, much of the hydrogen peroxide is expected to be generated by radiolysis of water which is exposed to fission fragments in the fuel rod. In this experiment, the concentrations of hydrogen peroxide in water were 1, 5, 10 and 30 vol.%. The gas stoichiometries (H/O ratios) in 1, 5, 10 and 30 vol.%  $\text{H}_2\text{O}_2$  atmospheres are calculated as 1.9978, 1.9888, 1.9767 and 1.9158, respectively. The oxygen potential ( $\Delta\bar{G}_{\text{O}_2}$ ) as a function of H/O ratio was calculated by using the thermodynamic calculation code (SOLGASMIX) [9]. The oxygen potential increases with the concentrations of hydrogen peroxide. The oxygen potentials in 1, 5, 10 and 30 vol.%  $\text{H}_2\text{O}_2$  at  $1000^\circ\text{C}$  are  $-100$ ,  $-83.3$ ,  $-73.8$  and  $-59.3$  kJ/mol, respectively. Fig. 2 also shows the oxygen potential in the various  $\text{H}_2\text{O}_2/\text{H}_2\text{O}$  atmospheres. The

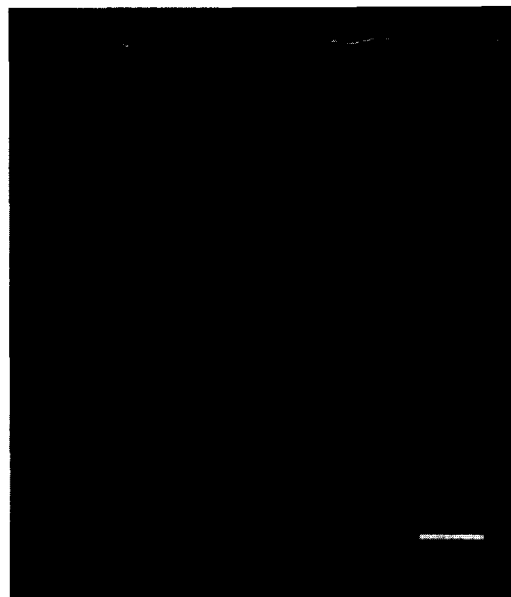


Fig. 3. Scanning electron micrograph of unirradiated fuel pellet after steam oxidation test at  $1000^\circ\text{C}$ .

oxygen potential at each temperature was evaluated from Fig. 2 and equilibrium O/U ratios in various atmospheres were derived using oxygen potential–O/U ratio diagrams [11].

### 3.2. Microstructural observations and oxygen analyses

After the steam oxidation tests, optical microstructural observations on polished surfaces of fuel pellets tested in 100%  $\text{H}_2\text{O}$  atmosphere were examined by optical and scanning electron microscopies. Fig. 3 shows a SEM image. No phase change to higher oxides is seen on the surface of the specimen and nor is precipitation of higher

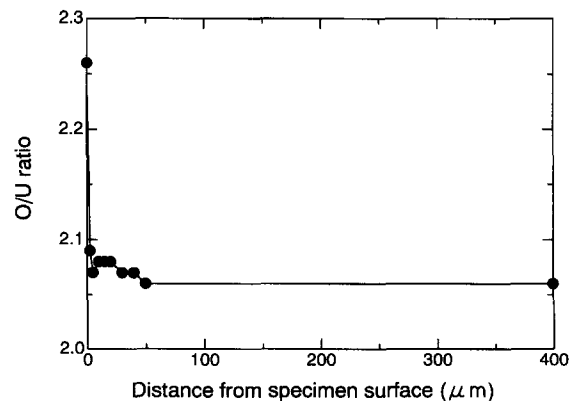


Fig. 4. O/U ratio distribution in  $\text{UO}_2$  fuel after steam oxidation tests at  $1000^\circ\text{C}$ .

oxides along the grain boundaries observed. The oxidation state is uniform. Fig. 4 shows the O/U ratio distribution analyzed by point analysis of EPMA. The local O/U ratio in the outermost region is 2.25 and the value corresponds to the single phase of  $U_4O_9$ . But the profiles of the O/U ratio in the inner region of the fuel specimens are almost flat and the values are equal to the O/U ratio after the oxidation tests. The EPMA results clearly show that the oxidation process is controlled by a reaction at the solid/gas interface.

### 3.3. Steam oxidation

#### 3.3.1. Unirradiated fuels

Fig. 5 shows typical oxidation curves of unirradiated fuel pellets in pure steam. In the figure, only the data at two different temperatures of 800 and 1000°C are plotted. The higher the temperature is, the higher the oxidation rate is and the faster saturation occurs. The steam oxidation rate of fuel pellets increases with temperature. Based on the solid/gas interface reaction rate determining model that the steam oxidation process of the fuel pellets was controlled by a reaction at the solid/gas interface, the experimental data were analyzed. This model is expressed by

$$\frac{dC}{dt} = \frac{S}{V} k (C_b - C), \quad (1)$$

where  $k$  is the oxygen surface exchange coefficient (cm/s),  $C$  is the O/U ratio of the solid in  $UO_2$  and  $C_b$  is the equilibrium O/U ratio determined by the oxygen potential in the gas phase.  $S/V$  is the surface-to-volume ratio of the specimen ( $cm^{-1}$ ). Integrating Eq. (1) yields the next equation:

$$\frac{(C_b - C)}{(C_b - 2)} = 1 - \frac{\Delta W_{ox}}{\Delta W_{eq}} = \exp\left(-\frac{t}{\tau}\right), \quad (2)$$

where  $\Delta W_{eq}$  is the weight gain at equilibrium,  $\Delta W_{ox}$  is the

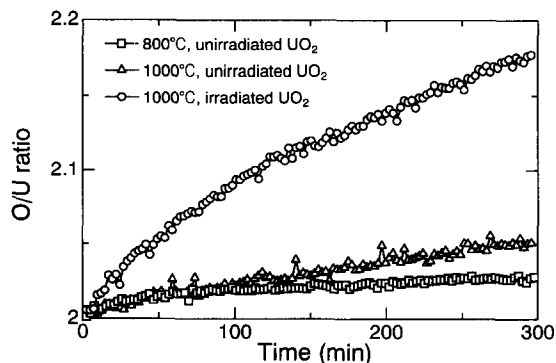


Fig. 5. Oxidation curves of unirradiated and irradiated  $UO_2$  fuel pellets.

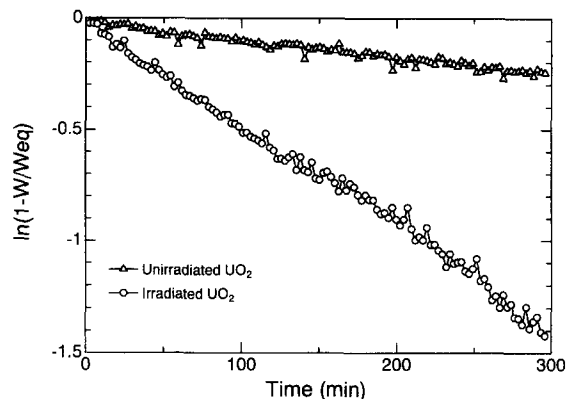


Fig. 6. Fit of experimental data to the phenomenological model.

weight gain of the specimen,  $t$  is time (s) and  $\tau$  is the characteristic time of the reaction ( $s^{-1}$ ).

The equilibrium O/U ratios in various atmospheres were derived using the established oxygen potential-O/U ratio diagram of  $UO_{2+x}$ , the higher oxides of  $U_4O_{9\pm y}$  and  $U_3O_{8-z}$ . The oxygen potentials were calculated using the thermodynamic code (SOLGASMIX) [9].  $\tau$  and  $k$  are obtained with the next equations:

$$\tau = \left(\frac{1}{k}\right) \left(\frac{V}{S}\right), \quad (3)$$

$$k = k_0 \exp\left(-\frac{E}{RT}\right), \quad (4)$$

where  $k_0$  is a pre-exponential factor,  $E$  is activation energy (J/mol),  $R$  is the gas constant ( $= 8.31433$  J/K/mol) and  $T$  is temperature (K). Fig. 6 shows a typical logarithmic plot of the weight change of the specimen at 1000°C. There is a straight line relationship between the logarithm of weight change and oxidation time. The slope in Fig. 6 is the reciprocal of the characteristic time ( $\tau$ ) of the reaction and hence the rate constant  $k$  can be calculated. The effective activation energy of the oxidation reaction can be evaluated from the reciprocal of the characteristic time and the reaction temperature.

Fig. 7 shows the Arrhenius plot of the surface exchange coefficient  $k$  calculated using Eq. (3). These resulting rate constants were compared with those reported by Cox et al. [3,4] and Abrefah et al. [5]. The values of this experiment are approximately one order of magnitude lower than their values. Two reasons for this can be considered: a difference in specific surface area ( $S/V$  ratio) and a difference in steam partial pressure. In this study, the specific surface area of the specimen was measured by using the BET method. On the other hand, the former studies used a geometrical specific surface area. Therefore the surface exchange coefficient  $k$  was also evaluated using the geometric  $S/V$  ratio of specimen in this experiment. The

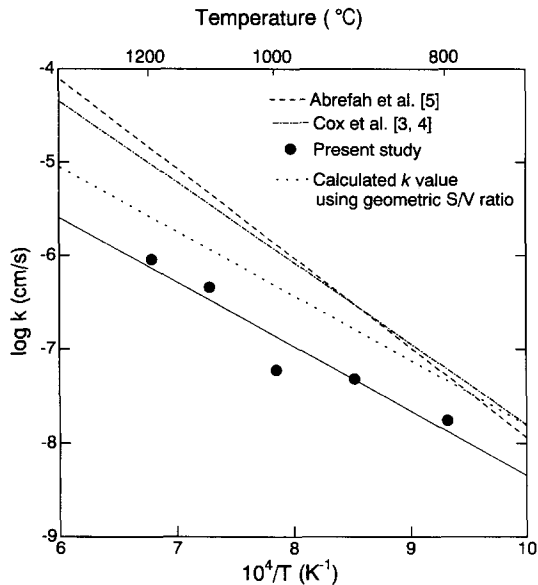


Fig. 7. Arrhenius plot for oxygen surface exchange coefficient of unirradiated fuel pellets.

re-calculated surface exchange coefficient  $k$  is shown with the dotted line in Fig. 7. The dotted line evaluated using the geometric  $S/V$  ratio is still a little lower than the values of Cox et al. and Abrefah et al. According to Abrefah et al. [5], the surface exchange coefficient  $k$  is proportional to the square root of steam partial pressure. The steam partial pressure in this experiment was 0.12 atm. On the other hand, Cox et al. and Abrefah et al. used 1 atm of the steam partial pressure. The difference in this steam partial pressure might have an influence on the  $k$  value. The  $k$  value of this experiment at  $P_{\text{H}_2\text{O}} = 1$  atm becomes  $2.89 (= \sqrt{1/0.12})$  times which is almost equal to values of Cox et al. and Abrefah et al.

The activation energy of this experiment is 132 kJ/mol and the pre-exponential factor is  $3.41 \times 10^{-2}$  cm/s. The oxygen surface exchange coefficient  $k$  in pure steam of 0.12 atm is explained with the following equation:

$$k \text{ (cm/s)} = 3.41 \times 10^{-2} \exp\left(-\frac{132 \times 10^3}{RT}\right). \quad (5)$$

### 3.3.2. Irradiated fuels

Fig. 5 also shows the oxidation curve of irradiated fuel pellets (burnup: 27 GWd/tU) in 100%  $\text{H}_2\text{O}$  at 1000°C. The increasing rate of O/U ratio in the irradiated pellets seems to be faster than that in the unirradiated pellets. Fig. 6 also shows a good straight line relationship between oxidation time and the logarithm of the weight change of specimen at 1000°C. This linearity means the surface-to-volume ratio of the specimen does not change during the

steam oxidation test and the formation of a grain boundary connection does not occur. It also means the steam oxidation of irradiated  $\text{UO}_2$  pellets is still controlled by a reaction at the solid/gas interface. Assuming that the oxygen surface exchange coefficient  $k$  of irradiated fuel is equal to that of unirradiated fuel, the surface-to-volume ratio of irradiated  $\text{UO}_2$  pellet was evaluated by using Eq. (3). The surface-to-volume ratio ( $S/V$  ratio) of irradiated  $\text{UO}_2$  pellets taken from the pellet outer region is  $555 \text{ cm}^{-1}$  and is approximately 2.6 times that of unirradiated fuel pellets.

### 3.4. Effect of liberated hydrogen

To evaluate the influence of liberated hydrogen, steam oxidation test in Ar–0.2% $\text{H}_2$  mixed gas was conducted at 1200°C, using unirradiated pellets. The equilibrium O/U ratio in Ar/0.2% $\text{H}_2/\text{H}_2\text{O}$  gas is lower than that in 100%  $\text{H}_2\text{O}$  atmosphere. From the oxygen potential diagram (Fig. 2), the oxygen potential is  $-215 \text{ kJ/mol}$  at 1200°C, so that the equilibrium O/U ratio is calculated as 2.014. There is a good agreement between the O/U ratio obtained in Ar/0.2% $\text{H}_2/\text{H}_2\text{O}$  gas test and the calculated one. The characteristic time of the reaction ( $\tau$ ) in Ar/0.2% $\text{H}_2/\text{H}_2\text{O}$  mixtures was evaluated from the relationship between the logarithm of the weight change of specimen and the oxidation time. The oxygen surface exchange coefficient  $k$  in 0.2% $\text{H}_2/\text{H}_2\text{O}$  atmosphere at 1200°C calculated using Eq. (3) is  $7.94 \times 10^{-7}$  (cm/s). On the other hand, the  $k$  value in 100%  $\text{H}_2\text{O}$  is  $7.11 \times 10^{-7}$  (cm/s). This shows that the liberated hydrogen has no effect on the steam oxidation rate constant.

### 3.5. Effect of hydrogen peroxide

Fig. 8 shows changes of the O/U ratio of unirradiated  $\text{UO}_2$  pellets in argon/steam/hydrogen peroxide mixtures at 1000°C for 5 h. The concentrations of hydrogen perox-

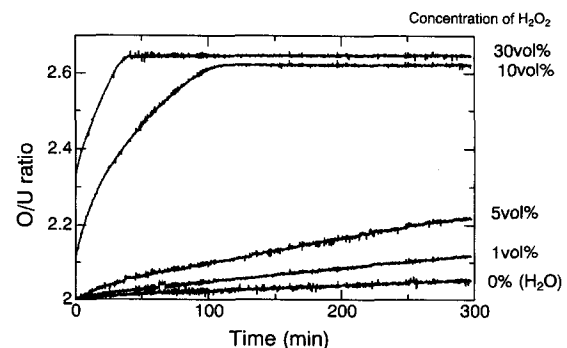


Fig. 8. Oxidation curve of unirradiated  $\text{UO}_2$  fuel pellets in  $\text{H}_2\text{O}_2/\text{H}_2\text{O}$  mixtures at 1000°C.

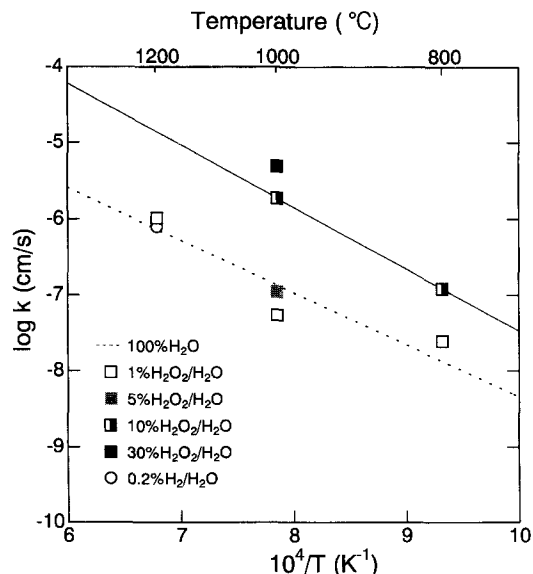


Fig. 9. Effect of liberated hydrogen and hydrogen peroxide on oxygen surface exchange coefficient.

ide in the bubbler were 1, 5, 10 and 30 vol.%. The oxidation rate is faster when increasing the concentrations of hydrogen peroxide. In the cases of more than 10 vol.% hydrogen peroxide, the increase in the O/U ratio occurs before the experimental temperature of 1000°C was reached and the O/U ratio arrived at the equilibrium value in less than 2 h. The equilibrium O/U ratios are almost equal to the calculated ones.

Fig. 9 summarizes the Arrhenius plot of surface exchange coefficient  $k$  in argon/steam/hydrogen peroxide mixtures calculated using Eq. (3) and the result in 100%  $\text{H}_2\text{O}$  atmosphere. When the concentrations of hydrogen peroxide were less than 5 vol.%, the oxygen surface exchange coefficient  $k$  is almost equal to that in 100%  $\text{H}_2\text{O}$  atmosphere. On the other hand, when the concentrations of hydrogen peroxide were more than 10 vol.%, the surface exchange coefficient  $k$  is higher than in 100%  $\text{H}_2\text{O}$  atmosphere. In comparison with the surface exchange coefficient  $k$  in 100%  $\text{H}_2\text{O}$  atmosphere, the  $k$  values in 10 and 30 vol.%  $\text{H}_2\text{O}_2$  increase approximately 14 and 37 times, respectively. When the concentration of  $\text{H}_2\text{O}_2$  is high, the hydrogen peroxide molecules which are not at thermal equilibrium, may reach the surface of the specimen. It is thought that these hydrogen peroxide molecules accelerate the decomposition of steam and the  $k$  value gets greater.

The activation energy in 10 vol.%  $\text{H}_2\text{O}_2$  atmosphere is 156 kJ/mol and the pre-exponential factor is 4.56 cm/s. The former value is a little larger than that obtained in pure steam. The oxygen surface exchange coefficient  $k$  in

10 vol.%  $\text{H}_2\text{O}_2$  atmosphere is explained with the following equation:

$$k \text{ (cm/s)} = 4.56 \exp\left(-\frac{156 \times 10^3}{RT}\right). \quad (6)$$

#### 4. Conclusion

Steam oxidation tests in the range of 800–1200°C in various atmospheres were conducted using unirradiated and irradiated  $\text{UO}_2$  pellets. The O/U ratio change was evaluated from weight gain of specimen. Results are summarized in the following.

(1) The O/U distribution in oxidized specimens analyzed by EPMA showed almost flat profiles. This indicated that the steam oxidation process was controlled by a reaction at the solid/gas interface, and not by oxygen diffusion in the solid.

(2) The oxygen surface exchange coefficient,  $k$ , as a function of temperature and atmosphere, was obtained. The presence of small amounts of hydrogen in steam decreased only the equilibrium O/U ratio, due to the low oxygen potential in this atmosphere, but had no effect on the  $k$  value. On the other hand, the  $k$  values obtained in  $\text{H}_2\text{O}_2/\text{H}_2\text{O}$  mixed gases increased drastically when the concentration of hydrogen peroxide in water was more than 10 vol.%. Finally, the  $k$  value was expressed with the following equations.

- In 100%  $\text{H}_2\text{O}$  atmosphere,

$$k \text{ (cm/s)} = 3.41 \times 10^{-2} \exp\left(-\frac{132 \times 10^3}{RT}\right).$$

- In 10 vol.%  $\text{H}_2\text{O}_2/\text{H}_2\text{O}$  atmosphere,

$$k \text{ (cm/s)} = 4.56 \exp\left(-\frac{156 \times 10^3}{RT}\right).$$

(3) The steam oxidation process of irradiated  $\text{UO}_2$  pellet was also controlled by a reaction at the solid/gas interface. When considering that the oxygen surface exchange coefficient  $k$  of irradiated fuel was equal to that of unirradiated fuel, the surface-to-volume ratio ( $S/V$  ratio) of irradiated  $\text{UO}_2$  pellet was approximately 2.6 times that of unirradiated fuel pellets.

#### References

- [1] K. Une, M. Imamura, M. Amaya, Y. Korei, J. Nucl. Mater. 223 (1995) 40.
- [2] J.T. Bittel, L.H. Sjdahl, J.F. White, J. Am. Ceram. Soc. 52 (1969) 466.
- [3] D.S. Cox, F.C. Iglesias, C.E.L. Hunt, N.A. Keller, R.D. Barrand, J.R. Mitchell, R.F. O'Connor, NUREG/CP-0078, 1986, p. 2.

- [4] D.S. Cox, R.F. O'Conner, W.W. Smeltzer, *Solid State Ionics* 53 (1992) 238.
- [5] J. Abrefah, A. de Aguiar Braid, W. Wang, Y. Khalil, D.R. Olander, *J. Nucl. Mater.* 208 (1994) 98.
- [6] B.J. Lewis, F.C. Iglesias, D.S. Cox, E. Gheorghiu, *J. Nucl. Mater.* 207 (1993) 228.
- [7] Y.H. Koo, D.S. Shon, Y.K. Yoon, *J. Korean Nucl. Soc.* 26 (1994) 90.
- [8] B.J. Lewis, F.C. Iglesias, D.S. Cox, E. Gheorghiu, *Nucl. Technol.* 92 (1990) 353.
- [9] T. M. Besmann, ORNL/TM-5775, Apr. 1977.
- [10] J. Takagi, K. Ishiguro, *Nucl. Sci. Eng.* 89 (1985) 177.
- [11] T. Matsui, thesis for the degree of D. Eng. of Nagoya University (1974).